Vol 16 No 3, March 2007
1009-1963/2007/16(03)/0826-08

Chinese Physics

© 2007 Chin. Phys. Soc.
and IOP Publishing Ltd

The upper critical field in two-band layered superconductors*

Liu Min-Xia(刘敏霞) and Gan Zi-Zhao(甘子钊)†

School of Physics, State Key Laboratory for Mesoscopic Physics, Peking University, Beijing 100871, *China*

(Received 27 July 2006; revised manuscript received 14 September 2006)

The upper critical field of clean MgB_2 is investigated using the two-band layered Ginzburg–Landau (GL) theory. The calculated results are fitted to the experimental data of clean MgB_2 crystal very well in a broad temperature range. Based on the GL theory for clean superconductors, a phenomenological theory for dirty superconductor is proposed. Selecting appropriate parameters, two-band layered GL theory is successfully applied to the crystal of $Mg(B_{1-x}C_x)_2$ and the neutron irradiation samples of MgB_2.

Keywords: MgB_2, Ginzburg–Landau theory, the upper critical field
PACC: 7420D, 7470, 7460E

1. Introduction

Since the discovery of superconductivity in MgB_2 at about 39 K in 2001,[1] MgB_2 has been studied widely. A large number of experimental[2−6] and theoretical[7,8] works indicate that MgB_2 has two gaps. The two gaps correspond to two distinct groups of bands. One is derived from σ antibonding p_{xy} B orbitals which form two hole-type two-dimensional (2D) deformed cylindrical Fermi surface (FS) sheets; the other from π bonding and antibonding p_z B orbitals which form two 3D near isotropic FS sheets. The coupling between the holes in the σ- band and the phonons is very strong and results in a larger energy gap.

The influence of doping or introducing defects on the superconductivity of MgB_2 has attracted a lot of interest. Doping or introducing defects can enhance the upper critical field (H_{c2}), reduce the anisotropy ratio of the upper critical field γ_H, form pinning centres and increase the critical current density J_c.[9−14] The impurities coming from doping or introducing defects have two effects. On the one hand, they change the band filling, the density of states (DOS) at the Fermi level E_F and the anisotropy of FS, resulting in the changes of the critical temperature (T_c) and the parameters in GL theory. On the other hand, they induce the charge carrier scattering. In two-band superconductors, there are two types of carriers scattering: intraband scattering and interband scattering. The intraband nonmagnetic impurity scattering does not affect the critical temperature, but it decreases the mean free path of the charge carriers. When the mean free path of the charge carriers becomes shorter than or comparable to the coherence length, the effective coherence length becomes shorter, leading to an increase of the upper critical field. The interband impurity scattering has a pair-breaking effect, causing a decrease of T_c and the merging of the two gaps. However, the interband impurity scattering in MgB_2 is weak due to the different parity of σ- and π- band wave functions,[15] so the intraband scattering dominates the superconductivity of MgB_2. As is known, the wavefunction of the carriers in the σ-band concentrates mainly in the B-layers, while the wavefunction of the carriers in the π- band mainly in both sides of the B-layers and is closer to the Mg-layers. Therefore, the different substitutional impurities have different effects on the intraband scattering within the σ- and π- bands. In previous works, the effects of C and Al doping on the superconductivity of MgB_2 have been studied in detail.[9−11,16−20]

The purpose of this paper is to study the effect of doping or introducing defects on the superconductivity of MgB_2 based on the two-band layer GL theory. There have been many papers about the GL theory for describing MgB_2.[21−25] Some indicate that the applicability of the GL approach to MgB_2 is limited to

*Project supported by the National Basic Research Program of China (973 Program) (Grant No 2006CB601002).
†Corresponding author. E-mail: zzgan@mail.phy.pku.edu.cn

an extremely narrow temperature range near T_c, because the c-axis coherence length in the σ- band is much smaller than that in the π- band.[26,27] Based on Refs.[26] and [27], we adopt a different treatment for the two-band GL theory, which broadens the temperature range of the applicability of the GL theory to MgB_2.

This article mainly concentrates on calculating H_{c2} and discussing the relations between H_{c2} and the parameters based on the two-band layered GL theory. The paper is organized as follows. In Section 2, the two-band layered GL equations are derived. In Section 3, these equations are used to derive the upper critical field and its anisotropy in clean limit. In Section 4, the two-band layered GL theory are applied to the upper critical field in dirty limit by changing the parameters.

2. Two-band layered GL theory

Considering the layered structure of MgB_2 and the characteristic of the wavefunction of carriers in the σ- and π- bands, we introduce the two-band layered GL theory. The GL free-energy function for two-band layered superconductors[24] can be written as:

$$F = \sum_n s \int (F_{1,n} + F_{2,n} + F_{12,n}) \mathrm{d}x\mathrm{d}y + \int \frac{H^2}{8\pi} \mathrm{d}V, \tag{1}$$

where z axis lies along the c crystallographic axis and n is the layer index. s denotes the distance between adjacent B-layers. Indices 1 and 2 correspond to the σ- and π- bands respectively. Index 12 corresponds to the interband interaction. $\boldsymbol{H}$ is the external magnetic field and $\boldsymbol{H} = \mathrm{curl}\boldsymbol{A}$, where $\boldsymbol{A} = (A_x, A_y, A_z)$ is the vector potential. Here

$$F_{i,n} = -\alpha_i |\Psi_{i,n}|^2 + \frac{1}{2}\beta_i |\Psi_{i,n}|^4 + \frac{\hbar^2}{2m_i} \left| \left(-\mathrm{i}\vec{\nabla}_2 - \frac{2e}{c\hbar}\boldsymbol{A}_2\right) \Psi_{i,n} \right|^2 + \frac{\hbar^2}{m_{iz}s^2} |\Psi_{i,n} - \Psi_{i,n+1} \exp(\mathrm{i}\chi_{n,n+1})|^2, \quad (i = 1, 2), \tag{2}$$

$$F_{12,n} = R_{12}(\Psi_{1,n}^* \Psi_{2,n} + \mathrm{C.C.}) + \frac{\hbar^2}{2m_{12}} \left\{ \left[\left(-\mathrm{i}\vec{\nabla}_2 - \frac{2e}{c\hbar}\boldsymbol{A}_2\right) \Psi_{1,n} \right]^* \left[\left(-\mathrm{i}\vec{\nabla}_2 - \frac{2e}{c\hbar}\boldsymbol{A}_2\right) \Psi_{2,n} \right] + \mathrm{C.C.} \right\} + \frac{1}{2} r_{12} \left\{ [\Psi_{1,n} - \Psi_{1,n+1} \exp(\mathrm{i}\chi_{n,n+1})]^* [\Psi_{2,n} - \Psi_{2,n+1} \exp(\mathrm{i}\chi_{n,n+1})] + \mathrm{C.C.} \right\}, \tag{3}$$

with

$$\vec{\nabla}_2 = \left(\frac{\partial}{\partial x}, \frac{\partial}{\partial y}, 0\right), \quad \boldsymbol{A}_2 = (A_x, A_y, 0), \quad \chi_{n,n+1} = \frac{2e}{c\hbar} \int_{z_n}^{z_{n+1}} A_z \mathrm{d}z, \tag{4}$$

where z_n is the z axial coordinate of the nth B layer and $z_{n+1} - z_n = s$; α_i, β_i, m_i, m_{iz}, R_{12}, m_{12} and r_{12} are the introduced parameters in GL theory.

In Eq.(1), $F_{1,n}$ and $F_{2,n}$ denote the GL free energy density of the carriers in the σ- and π- bands without interband interaction, F_{12} denotes the free energy density coming from the interband interaction. Comparing with the single-band GL free energy function, it is known that the first three terms in F_{1n} (F_{2n}) describe the free energy of σ- (π-) band in the nth layer and the fourth term is inter-layer interaction of σ- (π-) band. In $F_{12,n}$, the first and second terms describe the interband interaction in the nth layer and the third term is the inter-layer interband interaction. In this work, we neglect the second and third terms in $F_{12,n}$ and retain only the first term, i.e., the interband interaction in the same layer. These omissions can be justified by the microscopic theory.[22]

Supposing the magnetic field inclines by an angle θ with respect to the z axis in the yz plane, the magnetic field can be written as $\boldsymbol{H} = (0, H_y, H_z) = (0, H\sin\theta, H\cos\theta)$. We can choose the vector potential $\boldsymbol{A} = (0, H_z x, -H_y x)$. Using the same method as for single-band layered superconductor,[28] i.e., assuming $\Psi_{i,n}(x, y) = \exp[\mathrm{i}(Qy + \varphi_{i,n})] f_i(x)$, the GL equations for two-band layered superconductors can be reduced to the following form:

$$\begin{pmatrix} D_{11} & D_{12} \\ D_{21} & D_{22} \end{pmatrix} \begin{pmatrix} f_1 \\ f_2 \end{pmatrix} + \begin{pmatrix} \beta_1|f_1|^2 & 0 \\ 0 & \beta_2|f_2|^2 \end{pmatrix} \begin{pmatrix} f_1 \\ f_2 \end{pmatrix} = 0, \tag{5}$$

where

$$D_{ii}f_i = -\frac{\hbar^2}{2m_i}\frac{\partial^2}{\partial x^2}f_i + \left\{\frac{1}{2}m_i\omega_{iz}^2(x-x_Q)^2 + \frac{\hbar^2}{m_{iz}s^2}\left[1-\cos\left(\frac{2\pi}{\Phi_0}H_y s(x-x_Q)\right)\right] - \alpha_i\right\} f_i, \tag{6}$$

$$D_{12} = D_{21} = R_{12}, \tag{7}$$

with $x_Q = (e\Phi_0 Q/2\pi H_z|e|)$, $\omega_{iz} = 2|e|H_z/m_i c$; and $\Phi_0 = (ch/2e)$ is the magnetic flux quantum.

$D_{ii}f_i$ is similar to the Hamiltonian for a particle of effective mass m_i bound in a potential field;

$$V_i = \frac{1}{2}m_i\omega_{iz}^2(x-x_Q)^2 + \frac{\hbar^2}{m_{iz}s^2}\left[1-\cos\left(\frac{2\pi}{\Phi_0}H_y s(x-x_Q)\right)\right] - \alpha_i. \tag{8}$$

V_i is schematically plotted in Fig.1.

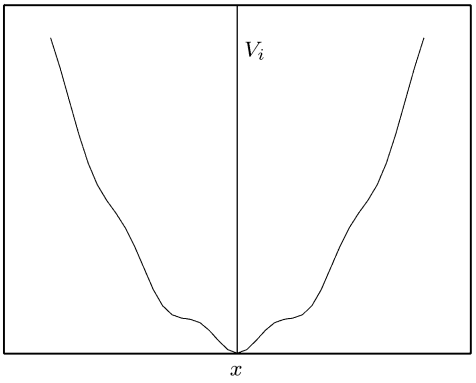


Fig.1. The schematic plot of the potential field V_i.

Obviously, its energy spectrum has a minimum. The solvability condition of Eq.(5) requires that the minimum eigenvalue of the following equation

$$\begin{pmatrix} D_{11} & D_{12} \\ D_{21} & D_{22} \end{pmatrix} \begin{pmatrix} f_1 \\ f_2 \end{pmatrix} = E \begin{pmatrix} f_1 \\ f_2 \end{pmatrix} \tag{9}$$

is less than zero. Equation (8) indicates that the energy levels will move upward with the increase of H. As a result, the upper critical field corresponds to the magnetic field when the minimum eigenvalue of Eq.(9) is equal to zero.

3. The upper critical field of two-band superconductors

3.1. The upper critical field in the c-direction

In this case $H_z = H$ and $H_y = 0$, thus we have

$$D_{ii}f_i = \left(-\frac{\hbar^2}{2m_i}\frac{\partial^2}{\partial x^2} + \frac{1}{2}m_i\omega_i^2 x^2 - \alpha_i\right) f_i, \tag{10}$$

$$D_{12}f_2 = R_{12}f_2, \quad D_{21}f_1 = R_{12}f_1, \tag{11}$$

with $\omega_i = 2|e|H/m_i c$. Equation (9) describes a system of two coupled oscillators. When the coupled term is neglected, the energy eigenvalues for each oscillator are given by

$$\epsilon_{i,j} = \left(j+\frac{1}{2}\right)\hbar\omega_i - \alpha_i, \ (j = 0, 1, 2, \ \dots\ ). \tag{12}$$

The coupled term is R_{12}, so only the energy levels with the same j can be coupled. The lowest coupled energy level comes from the coupling between two $j = 0$ levels of two oscillators. When $j = 0$, the energy levels of each oscillator are $\epsilon_{i,0} = \hbar\omega_i/2 - \alpha_i$ and their corresponding wavefunctions are

$$\begin{pmatrix} f_1 \\ f_2 \end{pmatrix} = \left(\frac{a_0}{\pi}\right)^{\frac{1}{4}} \mathrm{e}^{-a_0 x^2/2} \begin{pmatrix} c \\ d \end{pmatrix}, \tag{13}$$

where $a_0 = 2\pi H/\Phi_0$ and c, d are the variational parameters. The lowest coupled energy level is the solution of the following equation

$$\begin{pmatrix} \epsilon_{1,0} & R_{12} \\ R_{12} & \epsilon_{2,0} \end{pmatrix} \begin{pmatrix} c \\ d \end{pmatrix} = \epsilon \begin{pmatrix} c \\ d \end{pmatrix}, \tag{14}$$

and can be described as

$$\epsilon_m = \frac{1}{2}\left[(\epsilon_{1,0}+\epsilon_{2,0}) - \sqrt{(\epsilon_{1,0}-\epsilon_{2,0})^2 + 4R_{12}^2}\right]. \tag{15}$$

When $\epsilon_m = 0$, we can obtain the upper critical field

$$H_{c2} = \frac{\Phi_0}{2\pi\xi_{\rm eff}^2}, \tag{16}$$

where

$$\frac{1}{\xi_{\rm eff}^2} = \frac{1}{2}\left[\left(\frac{\alpha_1}{k_1}+\frac{\alpha_2}{k_2}\right) + \sqrt{\left(\frac{\alpha_1}{k_1}-\frac{\alpha_2}{k_2}\right)^2 + \frac{4R_{12}^2}{k_1k_2}}\right], \tag{17}$$

with $k_1 = \hbar^2/2m_1, k_2 = \hbar^2/2m_2$.

When the interband interaction is neglected, Eq.(5) is reduced to two independent single-band GL equations, corresponding to the critical temperatures T_{c1} and T_{c2} respectively. Then the parameters α_1 and α_2 can be approximately expressed as $\alpha_i = \alpha_{i0}(1 - T/T_{ci})$, where $T_{c1} > T_{c2}$, $\alpha_{10} > \alpha_{20}$ for MgB_2.[21] Now we can introduce the intrinsic coherence lengths $\xi_i^2 = k_i/\alpha_i$ for each band, so Eq.(17) is rewritten as

$$\frac{1}{\xi_{\rm eff}^2} = \frac{1}{2}\left[\left(\frac{1}{\xi_1^2}+\frac{1}{\xi_2^2}\right) + \sqrt{\left(\frac{1}{\xi_1^2}-\frac{1}{\xi_2^2}\right)^2 + \frac{4r^2}{\xi_{10}^2\xi_{20}^2}}\right], \tag{18}$$

where $r^2 = (R_{12}^2/\alpha_{10}\alpha_{20})$. $\xi_{10}^2 = k_1/\alpha_{10}$ and $\xi_{20}^2 = k_2/\alpha_{20}$ denote the intrinsic coherence lengths of the σ- and π- bands in the xy plane as $T \to 0$ respectively. Equation (18) indicates that $\xi_{\rm eff}$ is determined by the smaller coherence length if the interband interaction is neglected. When $H_{c2} = 0$ in Eq.(16), we can obtain the critical temperature of the superconductor

$$T_c = T_{c1} + \left[\frac{1}{2}(\sqrt{(T_{c1}-T_{c2})^2 + 4T_{c1}T_{c2}r^2} - (T_{c1}-T_{c2}))\right]. \tag{19}$$

This result is well known and indicates that the critical temperature T_c is higher than T_{c1}.

Equations (16) and (18) suggest that the value of $H_{c2}(T)$ depends on the parameters T_{c1}, T_{c2}, ξ_{10}, ξ_{20} and r^2. The theoretical result is shown in Fig.2 by the dashed line and the experimental data are taken from Ref.[29]. To fit the experimental data of Lyard *et al*,[29] we select the following parameters: $T_{c1} = 30.5\,\mathrm{K}$, $T_{c2} = 17.3\,\mathrm{K}$, $\xi_{10}^2 = 8.66\times10^{-17}\,\mathrm{m}^2$, $\xi_{20}^2 = 1.5\times10^{-16}\,\mathrm{m}^2$, $r^2 = 0.2$.

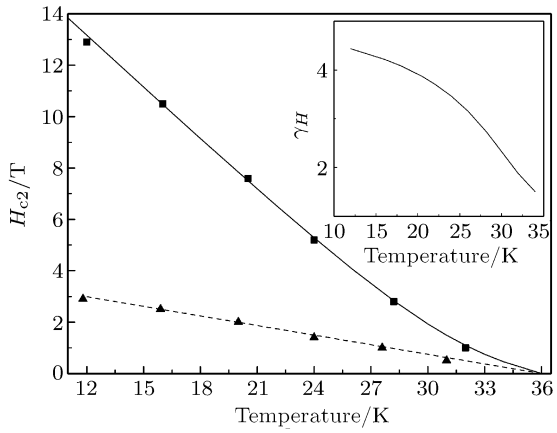


Fig.2. Magnetic phase diagram of the MgB_2 single crystals. The solid line and dashed line show the theoretical results H_{c2}^{ab} and H_{c2}^{c}, respectively. The experimental data are taken from Lyard *et al*[29] (symbols). The inset shows the anisotropy ratio γ_H.

3.2. The upper critical field for $\theta \neq 0$

In this case, $H_z = H\cos\theta$, $H_y = H\sin\theta$. If we regard Eq.(9) as the eigen equation of two coupled oscillators, the potential energy of each oscillator is the superposition of a simple harmonic potential energy and a periodic potential energy,

$$V_i = \frac{1}{2}m_i\omega_i^2\cos^2\theta x^2 + \frac{\hbar^2}{m_{iz}s^2}\sin^2\left(\frac{\pi H\sin\theta}{\Phi_0}sx\right). \tag{20}$$

Expanding V_i at the point of $x = 0$, we obtain

$$V_i \approx \frac{1}{2}m_i\left(\frac{2|e|H_{{\rm eff},i}}{m_ic}\right)^2 x^2, \tag{21}$$

where

$$H_{{\rm eff},i} = H\left(\cos^2\theta + \frac{m_i}{m_{iz}}\sin^2\theta\right)^{1/2}. \tag{22}$$

For MgB_2, the calculated results of energy band[30,31] are: $m_{1z}/m_1 \sim 40$ and $m_2/m_{2z} \sim (1 \sim 4)$. Since $s \sim 3.52$Å, the expansion of Eq.(21) is valid when $H < 100\,\mathrm{T}$. If the coupled term is neglected, the energy eigenvalues of each oscillator are equal to $\epsilon_{i,j} \approx (j+\frac{1}{2})\hbar\omega_i - \alpha_i$, where $\omega_i = 2|e|H_{{\rm eff},i}/m_ic$. Since $H_{{\rm eff},1} \neq H_{{\rm eff},2}$, the variational lengths of the wave functions of the oscillators are different. Therefore, not only should we consider the coupling between the energy levels with the same j, but also the coupling between the energy levels with different j. To obtain

the minimum eigenvalue of the coupled oscillator, we follow a variational approach. We look for a solution in the form

$$f_1(x) = cg_1(x) = c\left(\frac{a}{\pi}\right)^{1/4}\exp\left(-\frac{a}{2}x^2\right),$$
$$f_2(x) = dg_2(x) = d\left(\frac{b}{\pi}\right)^{1/4}\exp\left(-\frac{b}{2}x^2\right), \quad (23)$$

where a, b, c, d are variational parameters. Introducing $\overline{D}_{il} = \langle g_i|D_{il}|g_l\rangle$, $(i,l=1,2)$, the minimum eigenvalue of the system is the solution of the following equation

$$\begin{pmatrix}\overline{D}_{11} & \overline{D}_{12}\\ \overline{D}_{21} & \overline{D}_{22}\end{pmatrix}\begin{pmatrix}c\\ d\end{pmatrix} = \epsilon\begin{pmatrix}c\\ d\end{pmatrix}. \quad (24)$$

The solution of Eq.(24) is

$$\epsilon_m = \frac{1}{2}\left[(\overline{D}_{11}+\overline{D}_{22}) - \sqrt{(\overline{D}_{11}-\overline{D}_{22})^2 + 4\overline{D}_{12}\overline{D}_{21}}\right]. \quad (25)$$

By minimizing ϵ_m

$$\frac{\partial\epsilon_m}{\partial a} = 0, \quad \frac{\partial\epsilon_m}{\partial b} = 0, \quad (26)$$

we can obtain a_m, b_m as functions of H. Substituting a_m, b_m into the following equation

$$\epsilon_m(H_{c2}, a_m, b_m) = 0, \quad (27)$$

we can obtain the upper critical field H_{c2}.

Introducing $L_H^2 = \Phi_0/2\pi H$, $F_i(\theta) = \cos^2\theta + \frac{m_i}{m_{iz}}\sin^2\theta$, Eqs.(26) and (27) are transformed to

$$\left[\frac{1}{2}\left(\frac{\xi_{20}}{L_H}\right)^2\left(\frac{F_2}{b_H}+b_H\right)-(1-\eta t_1)\right]\left(\frac{\xi_{10}}{L_H}\right)^2\left(1-\frac{F_1}{a_H^2}\right) = 2r^2\frac{b_H-a_H}{(b_H+a_H)^2}\sqrt{\frac{b_H}{a_H}}, \quad (28)$$

$$\left[\frac{1}{2}\left(\frac{\xi_{10}}{L_H}\right)^2\left(\frac{F_1}{a_H}+a_H\right)-(1-t_1)\right]\left(\frac{\xi_{20}}{L_H}\right)^2\left(1-\frac{F_2}{b_H^2}\right) = -2r^2\frac{b_H-a_H}{(b_H+a_H)^2}\sqrt{\frac{a_H}{b_H}}, \quad (29)$$

$$\left[\frac{1}{2}\left(\frac{\xi_{20}}{L_H}\right)^2\left(\frac{F_2}{b_H}+b_H\right)-(1-\eta t_1)\right]\left[\frac{1}{2}\left(\frac{\xi_{10}}{L_H}\right)^2\left(\frac{F_1}{a_H}+a_H\right)-(1-t_1)\right] = r^2\frac{2\sqrt{b_Ha_H}}{b_H+a_H}, \quad (30)$$

where $t_1 = T/T_{c1}$, $t_2 = T/T_{c2}$, $\eta = T_{c1}/T_{c2}$, $a_H = aL_H^2$, $b_H = bL_H^2$. From these equations, we can obtain a_H, b_H and H_{c2} as functions of T and θ.

In the following discussion, we select the same parameters as those in the preceding section and let $m_1/m_{1z} = 0.034$ and $m_2/m_{2z} = 1.33$ to fit the experimental data of Lyard *et al*.[29] In Fig.2, the $H_{c2}(T)$ at $\theta = 0$ (calculated in the preceding section) and $\theta = \pi/2$ are plotted. It can be seen that the theoretical results are fitted to the experimental data measured on MgB_2 very well in a wide temperature range. In Fig.3, the calculated values of $a_H(\theta)$, $b_H(\theta)$, $\sqrt{F_1(\theta)}$, $\sqrt{F_2(\theta)}$ at $T = 30\,\mathrm{K}$ are plotted. At $\theta = 0$, $a_H = b_H = \sqrt{F_1} = \sqrt{F_2} = 1$. At $\theta \neq 0$, $a_H \geq \sqrt{F_1}$, $b_H \leq \sqrt{F_2}$ and $a_H \neq b_H$. Therefore, it is clear that a proper treatment for the two-band GL theory can take into account the difference of coherence lengths for two bands in c axis. If we introduce $A = \frac{1}{2}\left(\frac{F_1}{a_H}+a_H\right)$, $B = \frac{1}{2}\left(\frac{F_2}{b_H}+b_H\right)$ and $C = \frac{2\sqrt{a_Hb_H}}{a_H+b_H}$, Eq.(30) has a formal solution for H_{c2}

$$\frac{1}{\xi_{ef}^2} = \frac{1}{2}\left[\left(\frac{1}{\xi_1^2A}+\frac{1}{\xi_2^2B}\right) + \sqrt{\left(\frac{1}{\xi_1^2A}-\frac{1}{\xi_2^2B}\right)^2+\frac{4r_{12}^2C}{(\xi_{10}^2A)(\xi_{20}^2B)}}\right], \quad (31)$$

which is similar to Eq.(18).

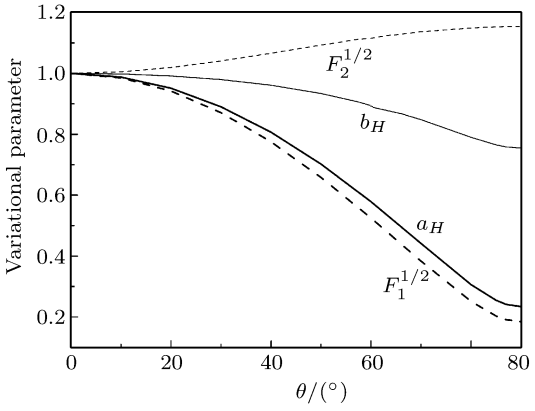


Fig.3. Angle dependence of variational parameters at $T = 30\,\mathrm{K}$ and the same set of GL parameters as those in Fig.2.

4. The upper critical field of dirty two-band superconductors

As has been discussed in the introduction, there are two effects of impurities or defects on superconductivity. Firstly, they shift the Fermi level, modify DOS at $E_{\rm F}$ and the band averaged Fermi velocities; secondly, they can increase carrier scattering. For MgB_2, the interband scattering is weak, so the superconductivity is dominated by the intraband scattering.

We also know that the more impurities the superconductor contains, the stronger the carrier scattering. The carrier scattering decreases the carrier mean free path ℓ. When the carrier mean free path is shorter than the corresponding coherence length in the clean superconductor, the superconductor becomes dirty and the coherence length becomes directly proportional to $(\hbar v_{\rm F}\ell/k_{\rm B}T_{\rm c})^{1/2}$ instead of $(\hbar v_{\rm F}/k_{\rm B}T_{\rm c})$. Here, $v_{\rm F}$ denotes the average Fermi velocity. For MgB_2, the intrinsic coherence lengths of each band become directly proportional to $(\xi_i\ell_i)^{1/2}$. Here, ℓ_i denotes the mean free path of the carriers in the i band. The intrinsic coherence lengths of each band decrease with the increase of the impurity concentration ρ. But this effect is different in the different band and different direction.

For the two-band superconductor MgB_2, the effects of intrinsic coherence lengths of each band on the upper critical field are different. Shown in Fig.4 are $H_{\rm c2}$ curves for different ξ_{10} and other parameters are the same as those in Fig.2. The set of parameters indicates that the impurities only affect the σ-band and reduce the anisotropy of the σ- band. From Fig.4, it can be seen that the two directional upper critical fields both increase considerably and the positive curvature of $H_{c2}^{ab}(t_1)$ becomes more obvious with the decrease of ξ_{10}, accompanied by a reduction in the anisotropy ratio γ_H. But γ_H still decreases with the increase of temperature. Figure 5 is another case, ξ_{20} and ξ_{2z0} are changed, but ξ_{20}/ξ_{2z0} and the other parameters are the same as those in Fig.2. This means that the impurities only enhance the scattering in the π-band, without affecting the anisotropy of the π-band. From Fig.5, it can be seen that with the decrease of the coherence length of the π-band, the two directional upper critical fields both increase lightly, the positive curvature of $H_{c2}^{ab}(t_1)$ in the vicinity of $T_{\rm c}$ gradually disappears and the curve of $H_{c2}^{c}(t_1)$ appears with an upward curvature at low temperature. When the impurity concentration is high, γ_H may increase with the increase of temperature in contrast to the clean superconductor MgB_2.

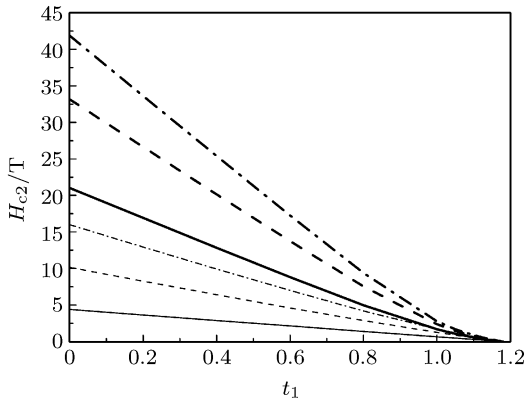


Fig.4. The curve of $H_{\rm c2}$ vs t_1 for $\xi_{10}^2 = 8.66 \times 10^{-17}{\rm m}^2$ (solid lines), $\xi_{10}^2 = 0.4 \times 8.66 \times 10^{-17}{\rm m}^2$ (dashed lines), $\xi_{10}^2 = 0.25 \times 8.66 \times 10^{-17}{\rm m}^2$ (dot-dashed lines). The thin lines and thick lines show the theoretical results $H_{\rm c2}^c$ and $H_{\rm c2}^{ab}$ respectively.

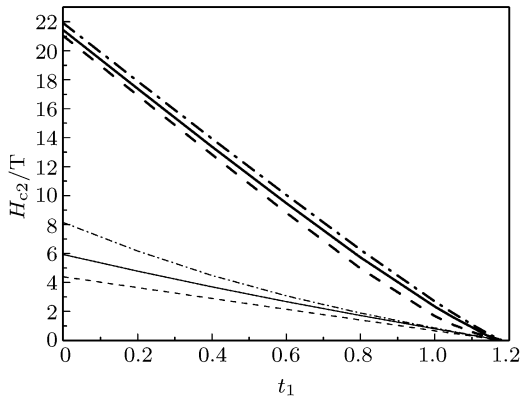


Fig.5. The curve of $H_{\rm c2}$ vs t_1 for $\xi_{20}^2 = 1.5 \times 10^{-16}{\rm m}^2$ (dashed lines), $\xi_{20}^2 = 0.4 \times 1.5 \times 10^{-16}{\rm m}^2$ (solid lines), $\xi_{20}^2 = 0.25 \times 1.5 \times 10^{-16}{\rm m}^2$ (dot-dashed lines). The thin lines and thick lines show the theoretical results $H_{\rm c2}^c$ and $H_{\rm c2}^{ab}$ respectively.

From Figs.4 and 5, we know that the σ-bands affect the upper critical field more strongly than the π-bands. As a result, we can enhance the upper critical field of MgB_2 by increasing the σ scattering. This possibility can be provided by the substitutions of B site by C, which is confirmed by many experimental works.[9−11] Reference [32] suggests that $H_{\rm c2}^{ab}(0)$ of $Mg(B_{1-x}C_x)_2$ thin film may approach ∼70T. The substitution of Mg site by Al mostly disturb the out-of-plane p_z orbitals of B, thus increases the π scattering.[33] From Fig.5, we know that the increase of the scattering in the π-band only enhances the upper critical field lightly. In Fig.5, we do not take into

account the first effect of impurities which reduces the upper critical field and destroys the superconductivity. In fact, the superconductivity of MgB_2 is determined by both of the two effects of impurities. Therefore, Al doping may decrease lightly or strongly change the upper critical field, which has been supported by a large number of experiments.[16−19]

In Figs.4 and 5, we neglect the change of the critical temperature. Actually, the impurities not only change the coherence length, but also suppress the critical temperature of the superconductor. Figure 6 plots the magnetic phase diagram of the $Mg(B_{1-x}C_x)_2$ single crystals with $x = 0.05$ (thin lines) and $x = 0.095$ (thick lines), and the experimental data are taken from the Ref.[10]. GL theory agrees well with the experimental result. Here, we use the following parameters: for $x = 0.05$: $T_c = 34.3\,K$; $\xi_{1z0}^2/\xi_{10}^2 = 0.048$; $\xi_{2z0}^2/\xi_{20}^2 = 1.286$; $\xi_{20}^2/\xi_{10}^2 = 3.112$; for $x = 0.095$: $T_c = 30.1\,K$; $\xi_{1z0}^2/\xi_{10}^2 = 0.059$; $\xi_{2z0}^2/\xi_{20}^2 = 1.28$; $\xi_{20}^2/\xi_{10}^2 = 3.62$. Because ξ_{20}^2/ξ_{10}^2 increase with ρ, C doping influences the σ-band more strongly than the π-band. It is consistent with the first principles electronic structure study on C-substituted MgB_2.[34] At the same time, due to the decrease of ξ_{1z0}^2/ξ_{10}^2, C doping reduces the anisotropy of σ-band leading to the decrease of γ_H.

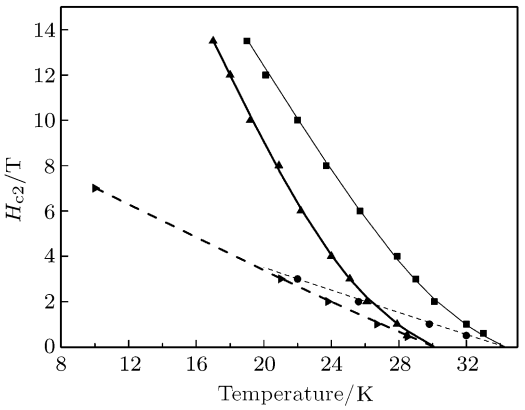


Fig.6. Magnetic phase diagram of the $Mg(B_{1-x}C_x)_2$ single crystals with $x = 0.05$ (thin lines) and $x = 0.095$ (thick lines). The solid lines and dashed lines show the theoretical results H_{c2}^{ab} and H_{c2}^{c}, respectively. The experimental data are taken from Ref.[10].

In Fig.7, we show the upper critical field of the neutron irradiation samples of the MgB_2 crystal. Here, the following parameters are used: for $F_n = 2 \times 10^{-21} m^{-2}$: $T_c = 37.3\,K$; $\xi_{1z0}^2/\xi_{10}^2 = 0.038$; $\xi_{2z0}^2/\xi_{20}^2 = 1.17$; $\xi_{20}^2/\xi_{10}^2 = 2.4$; for $F_n = 4 \times 10^{-21} m^{-2}$: $T_c = 36.5\,K$; $\xi_{1z0}^2/\xi_{10}^2 = 0.032$; $\xi_{2z0}^2/\xi_{20}^2 = 1$; $\xi_{20}^2/\xi_{10}^2 = 2.56$. From the above parameters, we can see that the effect of neutron irradiation on σ-band is almost of the same order as that on π-band, which is consistent with the experimental result.[35]

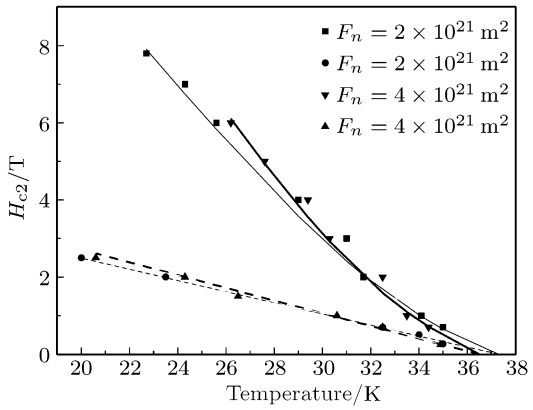


Fig.7. Magnetic phase diagram of the MgB_2 crystal after neutron irradiation. The solid lines and dashed lines show the theoretical results of H_{c2}^{ab} and H_{c2}^{c}, respectively. The experimental data are taken from Ref.[14].

5. Conclusions

In this paper, a method based on GL theory has been developed to study the upper critical field of two-band superconductors, particularly the MgB_2. In this method, the remarkable difference between the c-axis coherence length in σ-band and that in π-band can be taken into account. By selecting the appropriate values of parameters, the calculated results are fitted to the experimental data of clean MgB_2 crystal very well in a wide temperature range. For dirty two-band superconductors, a phenomenological model can consider the effect of impurities (defects) on the parameters, particularly the coherence lengths of the two bands. It is also shown, corresponding to the appropriate values of parameters, that the theoretical results are in good agreement with the data of $Mg(B_{1-x}C_x)_2$, $Mg_{1-x}Al_xB_2$ and the neutron irradiation samples of MgB_2 crystal well.

References

[1] Nagamatsu J, Nakagava N, Muranaka T, Zenitani Y and Akimitsu J 2001 *Nature (London)* **410** 63

[2] Iavarone M, Karapetrov G, Koshelev A E, Kwok W K, Crabtree G W and Hinks D G 2002 *Phys. Rev. Lett.* **89** 187002

[3] Schmidt H, Zasadzinski J E, Gray K E and Hinks D G 2002 *Phys. Rev. Lett.* **88** 127002

[4] Chen X K, Kostantinovic M J, Irwin J C, Lawrie K K and Franck J P 2001 *Phys. Rev. Lett.* **87** 157002

[5] Bouquet F, Fisher R A, Phillips N E, Hinks D G and Jorgensen J D 2001 *Phys. Rev. Lett.* **87** 047001

[6] Zhang J, Luo J L, Bai H Y, Chen Z J, Lin D H, Che G C, Ren Z A, Zhao Z X and Jin D 2002 *Acta Phys. Sin.* **51** 0342 (in Chinese)

[7] Liu A Y, Mazin I I and Kortus J 2001 *Phys. Rev. Lett.* **87** 087005

[8] Choi H J, Roundy D, Sun H, Cohen M L and Loule S G 2002 *Nature* **418** 758

[9] Lee S, Masui T, Yamamoto A, Vchiyama H and Tajima S 2003 *Physica* C **397** 7

[10] Kazakov S M, Puzniak R, Rogacki K, Mironov A V, Zhigadlo N D, Jun J, Soltmann Ch, Batlogg B and Karpinski J 2005 *Phys. Rev.* B **71** 024533

[11] Masui T, Lee S and Tajima S 2004 *Phys. Rev.* B **70** 024504

[12] Zhang X P, Ma Y W, Gao Z S, Yu Z G, Watanabe K and Wen H H 2006 *Acta Phys. Sin.* **55** 4873 (in Chinese)

[13] Putti M, Braccini V, Ferdeghini C, Gatti F, Grasso G, Manfrinetti P, Marre D, Palenzona A, Pallecchi I, Tarantini C, Sheikin I, Aebersold K V and Lehmann E 2005 *Appl. Phys. Lett.* **86** 112503

[14] Zehetmayer M, Eisterer M, Jun J, Kazakov S M, Karpinski J and Weber H W 2004 *Phys. Rev.* B **70** 214516

[15] Mazin I I, Andersen O K, Dolgov O V, Kortus J, Golubov A A, Kuz'menko A B and Van der Marel D 2002 *Phys. Rev. Lett.* **89** 107002

[16] Putti M, Braccini V, Ferdeghini C, Pallecchi I, Siri A S, Gatti F, Manfrinetti P and Palenzona A 2004 *Phys. Rev.* B **70** 052509

[17] Putti M, Ferdeghini C, Monni M, Pallecchi I, Tarantini C, Manfrinetti P, Palenzona A, Daghero D, Gonnelli R S and Stepanov V A 2004 cond-mat /0406377

[18] Kang B, Kim H J, Lee H S and Lee S I 2004 cond-mat /0403455

[19] Karpinski J, Zhigadlo N D, Schuck G, Kazakov S M, Batlogg B, Rogack K, Puzniak R, Jun J, Müller E, Wägli P, Gonnelli R, Daghero D, Ummarino G A and Stepanov V A 2005 *Phys. Rev.* B **71** 174506

[20] Angst M, Bud'ko S L, Wilker R H T and Canfield P C 2005 *Phys. Rev.* B **71** 144512

[21] Dao V H and Zhitomirsky M E 2005 cond-mat /0504053

[22] Zhitomirsky M E and Dao V H 2004 *Phys. Rev.* B **69** 054508

[23] Askerzade I N, Gencer A and Guclu N 2002 *Supercond. Sci. Technol.* **15** L13

[24] Askerzade I N 2005 *JETP Lett.* **81** 583

[25] Udomsamuthirun P, Changjan A, Kumvongsa C and Yoksan S 2005 *Physica* C **434** 62

[26] Koshelev A E and Golubov A A 2004 *Phys. Rev. Lett.* **92** 107008

[27] Golubov A A and Koshelev A E 2003 *Phys. Rev.* B **68** 104503

[28] Bulaevskii L N 1973 *Sov. Phys. JETP* **37** 1133

[29] Lyard L, Samuely P, Szabo P, Klein T, Mancenat C, Paulius L, Kim K H P, Jung C U, Lee H-S, Kang B, Choi S, Lee S-I, Marcus J, Blanchard S, Jansen A G M, Welp U, Karapetrov G and Kwock W K 2002 *Phys. Rev.* B **66** 180502

[30] Kong Y, Dolgov O V, Jepsen O and Andersen O K 2001 *Phys. Rev.* B **64** 020501

[31] Brinkman A, Golubov A A, Rogalla H, Dolgov O V, Kortus J, Kong Y, Jepsen O and Andersen O K 2002 *Phys. Rev.* B **65** 180517

[32] Braccini V, Gurevich A, Giencke J E, Jewell M C, Eom C B, Larbalestier D C, Pogrebnyakow A, Cui Y, Liu B T, Hu Y F, Redwing J M, Li Qi, Xi X X, Singh R K, Gandikota R, Kim J, Wilkens B, Newman N, Rowell J, Moeckly B, Ferrando V, Tarantini C, Marre D, Putti M, Ferdeghini C, Vaglio R and Haanappel E 2005 *Phys. Rev.* B **71** 012504

[33] Gurevich A 2003 *Phys. Rev.* B **67** 184515

[34] Kasinathan D, Lee K W and Pickett W E 2004 cond-mat /0409563

[35] Ortolani M, Dicastro D, Postorino P, Pallecchi I, Monni M, Putti M and Dore P 2005 *Phys. Rev.* B **71** 172508